Available online at www.sciencedirect.com
ScienceDirect
Renewable and Sustainable Energy Reviews
12 (2008) 824–838
RENEWABLE
& SUSTAINABLE
ENERGY REVIEWS
www.elsevier.com/locate/rser

A review of two-phase gas–liquid adiabatic flow characteristics in micro-channels

Sira Saisorn[a], Somchai Wongwises[b,*]

[a]*Energy Division, The Joint Graduate School of Energy and Environment, King Mongkut's University of Technology Thonburi, Bangmod, Bangkok 10140, Thailand*
[b]*Fluid Mechanics, Thermal Engineering and Multiphase Flow Research Laboratory (FUTURE), Department of Mechanical Engineering, King Mongkut's University of Technology Thonburi, Bangmod, Bangkok 10140, Thailand*

Received 7 July 2006; accepted 13 October 2006

Abstract

A literature review of recent research on two-phase flow in micro-channels is provided in this article. Researches on the micro-hydrodynamics concerned with two-phase gas–liquid adiabatic flow characteristics in both circular and non-circular micro-channels are discussed. This review aims to survey and identify new findings obtained from this attractive area, which may contribute to optimum design and process control of high performance miniature devices comprising extremely small channels. The results obtained from a number of previous studies show that the flow behaviors in the micro-channels deviate significantly from those in ordinarily sized channels. A clear understanding of the flow behaviors encountered is necessary to answer the fundamental questions related to the two-phase flow phenomena. Similar to the ordinarily sized channels, it is expected that the flow pattern, pressure drop and void fraction will influence the two-phase pressure drop, holdup, system stability, exchange rates of momentum, heat and mass during the phase-change heat transfer processes. It is obvious that publications available on micro-channels are relatively small compared to those for ordinarily sized channels and further systematic studies of two-phase gas–liquid adiabatic flow in micro-channels are required.

Keywords: Two-phase flow; Micro-channel; Flow characteristic

*Corresponding author. Tel.: +66 2 470 9115; fax: +66 2 470 9111.
E-mail address: somchai.won@kmutt.ac.th (S. Wongwises).

1364-0321/$ - see front matter
doi:10.1016/j.rser.2006.10.012

Contents

1. Introduction

In the past years, studies on two-phase flow and heat transfer characteristics in micro-channel flow passages have become more necessary due to the rapid development of micro-scale devices used for several engineering applications including medical devices, high heat-flux compact heat exchangers, and cooling systems of various types of equipment such as high performance micro-electronics, supercomputers, high-powered lasers, and so on.

In addition to the attractive phenomena caused by the significant role of the surface effects, this emerging field enables us to develop powerful miniature devices for operation in a domain which seemed to be unfeasible in the past. However, it is obvious that a comprehensive understanding is still lacking on the trends and parameters dominating the flow behavior in mini- and micro-channels. Thus, fundamental heat transfer and flow characteristics problems encountered in the development and processing of micro-electronic-mechanical systems (MEMS) have become a significant challenge for the design and control of these micro-systems. According to the requirement of new solutions for dissipating heat and keeping uniform temperature distributions in modern devices, a clear understanding of the major mechanisms affecting micro-scale heat transfer is essential for optimum design and process control of micro-systems.

The two-phase flow and heat transfer characteristics in small channels such as micro-channels and mini channels are likely to be strongly dependent on the surface tension effects in addition to viscosity and inertia forces resulting in significant differences in the two-phase flow phenomena between ordinarily sized channels and small channels. Several investigators have proposed the criterion for a small channel based on different dimensionless parameters.

Serizawa et al. [1] described the criterion for classification of micro-channel proposed by Suo and Griffith [2] as follows:

$$\frac{\lambda}{D} \geqslant 3.3, \tag{1}$$

where λ is the Laplace constant defined by

$$\lambda = \sqrt{\frac{\sigma}{g(\rho_L - \rho_G)}}. \tag{2}$$

Brauner and Moalem-Maron [3] proposed the different criterion as follows:

$$Eo \leqslant (2\pi)^2, \tag{3}$$

Nomenclature

C	parameter dependent on Reynolds number
C_0	distribution parameter
D	channel diameter, m
D_B	bubble diameter, m
D_e	equi-periphery diameter, m
D_h	hydraulic diameter, m
dP	pressure drop, Pa
dz	unit length, m
Eo	Etovos number
F	time fraction
f	friction factor
G	mass flux, $kg/s\,m^2$
g	gravitational acceleration, m/s^2
j	superficial velocity, m/s
KE_{avg}	two-phase mixture's average kinetic energy, $kg/m\,s^2$
L	length, m
n_1	1 for laminar flow; 0.25 for turbulent flow
n_2	1 for laminar flow; 0.25 for turbulent flow
Re	Reynolds number
s	channel gap, m
U	average velocity, m/s
V	rising bubble velocity relative to the liquid phase, m/s
We_v	Weber number for vapor
w	channel width, m
X	parameter defined by Eq. (30)
X_{ann}	parameter defined by Eq. (37)
x	flow quality
α	void fraction
α_m	mean void fraction
χ	Lockhart–Martinelli parameter
ϕ	two-phase multiplier
λ	Laplace constant
μ	dynamic viscosity, kg/m s
v	kinematic viscosity, m^2/s
ρ	density, kg/m^3
σ	surface tension, N/m

Subscripts

ann	annular flow regime
B	bubble; slug bubble
c	contraction
G	gas phase, vapor phase
GS	gas slug

I	gas–liquid interface
int	intermittent flow regime
L	liquid phase
LO	all-liquid
LS	liquid slug
liq	liquid flow regime
s	smaller channel
T	two-phase mixture
UC	unit cell
VO	all-vapor
vap	vapor flow regime

where Eo is the Etovos number defined by

$$Eo = \frac{g(\rho_L - \rho_G)D^2}{\sigma}. \tag{4}$$

From Eqs. (1)–(4), σ is surface tension, g is gravitational acceleration, D is channel diameter, ρ_L and ρ_G are liquid and gas densities, respectively.

Unfortunately, it is likely to be insufficient to identify the distinction between small channels and ordinarily sized channels by these equations. Some arbitrary channel classifications based on the hydraulic diameter D_h have been proposed. Recently, Mehendale et al. [4] employed the hydraulic diameter as an important parameter for defining the heat exchangers as follows:

- Micro-heat exchanger: $1\,\mu m \leqslant D_h \leqslant 100\,\mu m$
- Meso-heat exchanger: $100\,\mu m \leqslant D_h \leqslant 1\,mm$
- Compact heat exchanger: $1\,mm \leqslant D_h \leqslant 6\,mm$
- Conventional heat exchanger: $D_h > 6\,mm$

Based on the evolution of small flow channels used in engineering applications, however, Kandlikar [5] proposed the channel classification as follows:

- Conventional channels: $D_h > 3\,mm$
- Mini-channels: $200\,\mu m \leqslant D_h \leqslant 3\,mm$
- Micro-channels: $10\,\mu m \leqslant D_h \leqslant 200\,\mu m$

Although there have been a number of criteria based on the hydraulic diameter, the channel classifications available cannot relate the channel diameter to the fluid flow mechanisms. Further investigations should be conducted to meet a more general definition dealing with the channel classification.

To obtain an appropriate design and process control of the various engineering systems employing these small channels, the two-phase flow characteristics as well as heat transfer mechanisms in various small channels, especially for micro-channels, should be clarified. In the past decade, there has been a relatively small amount of publications available for micro-channels compared to those for ordinarily sized channels.

The aim of this paper is to present a review of the most common types of research works done on two-phase gas–liquid adiabatic flow characteristics in micro-channels, and to propose the areas available for further investigations.

2. Two-phase Gas–liquid adiabatic flow characteristics in micro-channels

Up to now, there have been publications dealing with two-phase gas–liquid adiabatic flow characteristics in micro-channels with various geometrical configurations. However, the two most common types of such configurations employed by previous researchers are circular and non-circular micro-channels.

2.1. Circular micro-channels

Adiabatic two-phase air–water flow characteristics, including the two-phase flow pattern as well as the void fraction and two-phase frictional pressure drop, in circular micro-channels were experimentally studied by Triplett et al. [6,7]. For flow visualization results corresponding to their first paper, the flow patterns observed were bubbly, slug, churn, slug-annular and annular. These experimental results were compared with other experimental data obtained from previous investigators. The two-phase flow pattern transitions generally disagreed with the lines calculated from the existing models and correlations.

According to their second paper, the measured values of void fraction and two-phase pressure drop in bubbly and slug flow regimes were found to be best predicted by the models based on the homogeneous mixture assumption. In the annular flow regime, however, the experimental void fractions and pressure drops were compared with the models as well as the available correlations, with poor agreement.

Kawahara et al. [8] used a circular fused silica micro-channel with a diameter of 100 μm to investigate two-phase flow characteristics. They observed many different flow patterns simultaneously in the circular channel under any given flow condition tested. Due to such simultaneous appearances, they used the probability of appearance of each flow pattern along with the time-averaged void fraction obtained from each flow condition to define the flow regimes as shown below.

- Slug-ring flow was defined when the probability of "thin liquid film" was greater than that of "ring liquid film" and the time-averaged void fraction was less than 0.8.
- Ring-slug flow corresponded to when the probability of "ring liquid film" was larger than that of "thin liquid film" and the time-averaged void fraction was less than 0.8.
- Semi-annular flow was associated with flow in which the flow alternated mostly between "liquid alone" and "ring liquid film". The time-averaged void fraction was greater than 0.8.
- Multiple flow included "liquid alone", "thin liquid film", "ring liquid film", "thick liquid film" and "deformed interface", and the time-averaged void fraction was less than 0.8.

The flow patterns defined were used to develop a flow pattern map which was subsequently compared to other flow regime maps existing for two-phase flow of air–water in ~1 mm diameter channels. It was noted that bubbly and churn flow patterns were absent in the experimental results due to the laminar nature of liquid flowing through the

micro-channel. The low value of the time-averaged void fraction, even at high gas flow rates, indicated the large slip ratios and weak momentum coupling between the phases. The friction factor in single-phase liquid flow and two-phase friction multiplier were also analyzed. The single-phase friction factor was found in reasonable agreement with the conventional correlation. The two-phase friction multiplier data correlated well with the Lockhart–Martinelli correlation based on a separated flow assumption, but the agreement between the data and homogeneous flow model was generally poor.

Chen et al. [9] experimentally studied the characteristics of adiabatic two-phase flow of nitrogen–water in glass tubes with two different diameters, 1.0 and 1.5 mm. Four common flow patterns including bubbly flow, slug flow, churn flow and annular flow were observed and a so-called bubble-train slug flow previously reported in a large channel under micro-gravity effects [10] was also observed and discussed in this work. The random manner of the number of bubbles counted in the bubble-train slug flow pattern was attributed to the turbulent nature. Moreover, increasing liquid superficial velocity tended to lower the number of bubbles. A modified drift flux model was found to be an appropriate approach to correlate bubble velocity for the three different flow patterns covering slug flow, bubble-train slug flow and churn flow. The correlation is expressed as

$$U_{\mathrm{B}} = 0.932 j_{\mathrm{T}}^{1.11}, \tag{5}$$

where U_{B} is bubble velocity and j_{T} is superficial velocity of the two-phase mixture.

Furthermore, the experimental void fractions were well predicted by the use of this modified drift flux model in conjunction with the following fundamental equation:

$$\alpha = \frac{j_{\mathrm{G}}}{U_{\mathrm{B}}}, \tag{6}$$

where α is void fraction and j_{G} is gas superficial velocity.

Serizawa et al. [1] investigated the visualization of the two-phase flow pattern in circular micro-channels. The flowing mixture of air and water in channels of 20, 25 and 100 μm in diameter and that of steam and water in a channel of 50 μm in diameter were conducted experimentally. Two-phase flow patterns obtained from both air–water and steam–water flows were quite similar and their detailed structures were described. The study confirmed that the surface wettability had a significant effect on the two-phase flow patterns in very small channels. It was also found that the air–water two-phase flow pattern transitions generally agreed with the lines predicted by the Mandhane's correlation and the cross-sectional average void fraction concerned with bubbly and slug flows followed the values obtained from the Armand correlation [11] for an air–water system.

Chung and Kawaji [12] performed an experiment in order to distinguish two-phase flow characteristics in micro-channels from those in mini-channels. Four different circular diameters ranging from 50 to 526 μm were employed to examine a scaling effect on nitrogen–water two-phase flow. The results including the flow patterns, void fraction and two-phase pressure drop were analyzed.

For larger tubes tested (250 and 526 μm), they observed flow patterns consistent with those obtained from mini-channels having diameters of around 1 mm. The corresponding flow patterns were bubbly, slug, churn, slug-annular and annular flow. The time-averaged void fraction agreed reasonably with the Armand-type correlation available for mini-channels. In the case of two-phase pressure drop, it was found that at a given

Lockhart–Martinelli parameter the two-phase friction multiplier tended to change with the variation of mass flux, similar to that appearing in mini-channels.

For relatively small channels (49.5 and 100 μm), only slug flow was observed under the experimental conditions tested. The void fraction and pressure drop characteristics were generally opposite to those of larger channels previously discussed. The relationship between the void fraction and volumetric quality was found to be non-linear and hence, the Armand-type correlation became unpredictable for these channel sizes. In addition, the frictional multiplier was independent of mass flux. Apparently, diameters between 100 and 250 μm seemed to be in the range causing the notable change in two-phase flow mechanisms. Additionally, they modified Garimella et al.'s [13] model to predict the two-phase pressure drop for micro-channels having diameters of less than 100 μm. In the proposed model, they assumed that the flow consisting of unit cells (UC) was completely intermittent as shown in Fig. 1. For each unit cell, there were two regions, including liquid single-phase flow region (or liquid slug), which had no entrained gas bubbles and the region occupied by the two-phase flow of liquid and gas. The latter region was formed by axially symmetrical gas slug surrounded by an annular liquid film with uniform thickness around the channel circumference. Because of the viscous effect, the velocity of the liquid film around the gas slug was assumed to be significantly low compared to that of liquid and gas slugs.

In the single-phase region, the pressure gradient in the liquid slug is evaluated from the Darcy–Weisbach equation:

$$\left(\frac{\mathrm{d}P}{\mathrm{d}z}\right)_{\mathrm{LS}} = f_{\mathrm{LS}}\frac{\rho_{\mathrm{L}} U_{\mathrm{LS}}^2}{2D}, \tag{7}$$

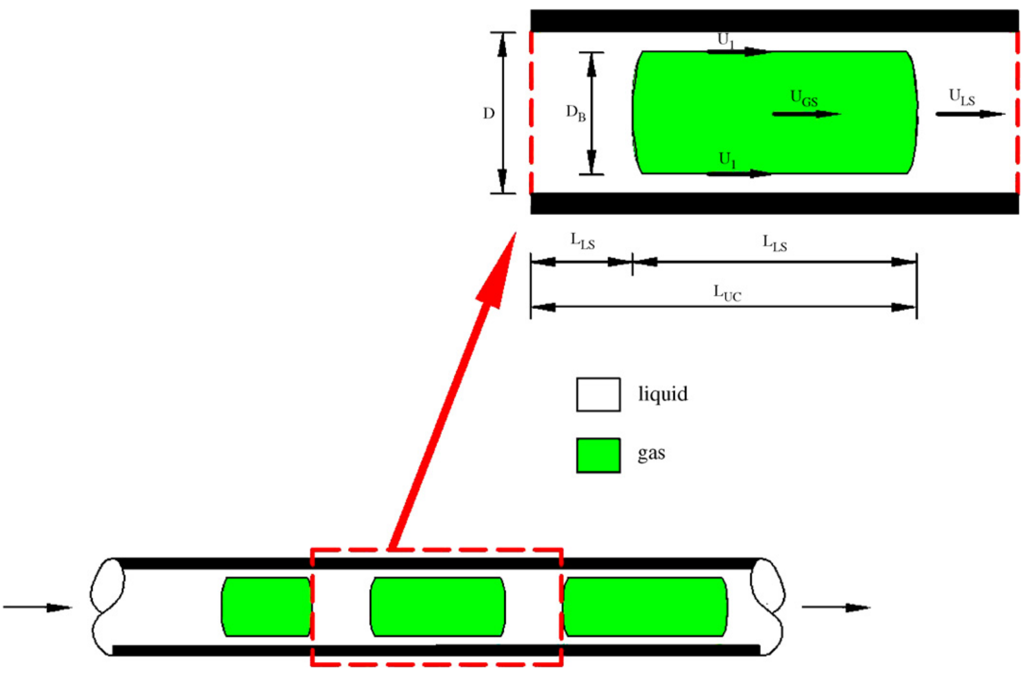

Fig. 1. Schematic diagram of unit cell for model of Chung and Kawaji [12].

where $(\mathrm{d}P/\mathrm{d}z)_{\mathrm{LS}}$ is the pressure gradient in the liquid slug, and f_{LS} is the friction factor for the liquid slug. The friction factor for fluid flow in a circular channel is given by

$$f_{\mathrm{LS}} = \frac{64}{Re_{\mathrm{LS}}}, \quad \text{for laminar flow } (Re_{\mathrm{LS}} \leqslant 2100), \tag{8}$$

$$f_{\mathrm{LS}} = \frac{0.3164}{Re_{\mathrm{LS}}^{0.25}}, \quad \text{for turbulent flow } (Re_{\mathrm{LS}} < 100{,}000) \text{ in a smooth channel.} \tag{9}$$

Eq. (9) is known as Blasius equation. In the model, it was noted that, for the transition from laminar to turbulent flow ($2100 < Re_{\mathrm{LS}} < 4000$), the Blasius formula was also employed to obtain the friction factor. The Reynolds number of the liquid slug, Re_{LS}, is defined as

$$Re_{\mathrm{LS}} = \frac{\rho_{\mathrm{L}} U_{\mathrm{LS}} D}{\mu_{\mathrm{L}}}, \tag{10}$$

where μ_{L} is the dynamic viscosity for liquid phase. In Eqs. (7) and (10), U_{LS} represents the average velocity of the liquid slug and is expressed by

$$U_{\mathrm{LS}} = \frac{j_{\mathrm{L}}}{1-\alpha}, \tag{11}$$

where j_{L} is the superficial liquid velocity.

In the two-phase region, the average velocity of the gas slug, U_{GS}, is taken to be equal to that of the gas phase, U_{G}

$$U_{\mathrm{GS}} = U_{\mathrm{G}} \tag{12}$$

and

$$U_{\mathrm{G}} = \frac{j_{\mathrm{G}}}{\alpha}. \tag{13}$$

The pressure gradient in the two-phase region, $(\mathrm{d}P/\mathrm{d}z)_{\mathrm{T}}$, is given by

$$\left(\frac{\mathrm{d}P}{\mathrm{d}z}\right)_{\mathrm{T}} = f_{\mathrm{GS}} \frac{\rho_{\mathrm{G}}(U_{\mathrm{GS}} - U_{\mathrm{I}})^2}{2D_{\mathrm{B}}}, \tag{14}$$

where f_{GS} represents the friction factor for the gas slug and the determination of f_{GS} is similar to that of f_{LS}. The Reynolds number of the gas slug, Re_{GS}, is given by

$$Re_{\mathrm{GS}} = \frac{\rho_{\mathrm{G}}(U_{\mathrm{GS}} - U_{\mathrm{I}}) D_{\mathrm{B}}}{\mu_{\mathrm{G}}}, \tag{15}$$

where μ_{G} is the dynamic viscosity for gas phase. U_{I} and D_{B} in Eqs. (14) and (15) represent the average velocity of the gas–liquid interface and bubble diameter, respectively. U_{I} is

defined by Chung and Kawaji [12] as follows:

$$U_{\mathrm{I}} = \frac{(\mathrm{d}P/\mathrm{d}z)_{\mathrm{T}}}{16\mu_{\mathrm{L}}}(D^2 - D_{\mathrm{B}}^2). \tag{16}$$

The bubble diameter is assumed to be

$$D_{\mathrm{B}} = 0.90D. \tag{17}$$

The unknown variables including Re_{GS}, U_{I}, and $(\mathrm{d}P/\mathrm{d}z)_{\mathrm{T}}$ are obtained through Eqs. (14)–(16). Finally, the total frictional pressure gradient, $(\mathrm{d}P/\mathrm{d}z)_{\mathrm{UC}}$, across the whole unit cell is expressed by

$$\left(\frac{\mathrm{d}P}{\mathrm{d}z}\right)_{\mathrm{UC}} = \left(\frac{\mathrm{d}P}{\mathrm{d}z}\right)_{\mathrm{T}}\frac{L_{\mathrm{GS}}}{L_{\mathrm{UC}}} + \left(\frac{\mathrm{d}P}{\mathrm{d}z}\right)_{\mathrm{LS}}\frac{L_{\mathrm{LS}}}{L_{\mathrm{UC}}}, \tag{18}$$

where the relative lengths of the gas slug ($L_{\mathrm{GS}}/L_{\mathrm{UC}}$) and liquid slug ($L_{\mathrm{LS}}/L_{\mathrm{UC}}$) are approximated by

$$\frac{L_{\mathrm{GS}}}{L_{\mathrm{UC}}} = \alpha\left(\frac{D}{D_{\mathrm{B}}}\right)^2, \tag{19}$$

$$\frac{L_{\mathrm{LS}}}{L_{\mathrm{UC}}} = 1 - \frac{L_{\mathrm{GS}}}{L_{\mathrm{UC}}}. \tag{20}$$

Based on the micro-channels having diameters of 100 and 50 μm, the experimental two-phase pressure drop data were predicted well by this slug flow model.

Coleman and Krause [14] carried out an experiment to measure R-134a two-phase pressure drops due to contraction in circular micro-channel headers. The measured two-phase pressure drops were considerably high compared to some existing correlations. However, the authors suggested that the use of model developed by Schmidt and Friedel [15] in conjunction with the momentum density model was in reasonable agreement with the measured data.

Two-phase air–water pressure changes in the circular channel, having sudden expansion and contraction sections, were experimentally studied by Abdelall et al. [16]. Two stainless steel tubes were connected to form such sections. The diameters of the larger tube and smaller tube were 1.6 and 0.84 mm, respectively. The two-phase pressure changes were found to be considerably small when compared to those predicted by the homogeneous flow model. This indicated significant velocity slip in the neighborhood of the flow disturbance resulting from the area change. On the other hand, the pressure change data were well predicted by a simple one-dimensional (1D) flow theory with the slip ratio model based on the ideal annular flow regime with minimum entropy generation. They also developed an empirical correlation of two-phase multiplier for the flow area

contraction, $\phi_{\mathrm{LO,c}}$:

$$\frac{\phi_{\mathrm{LO,c}}}{\chi} = 120(\chi\, Re_{\mathrm{LO,s}})^{-0.7}, \tag{21}$$

where $Re_{\mathrm{LO,s}}$ is the Reynolds number with the total flow in the liquid phase in smaller channel and the Lockhart–Martinelli parameter, χ, is expressed by

$$\chi = \left(\frac{\mu_{\mathrm{L}}}{\mu_{\mathrm{G}}}\right)^{0.1}\left(\frac{1-x}{x}\right)^{0.9}\left(\frac{\rho_{\mathrm{G}}}{\rho_{\mathrm{L}}}\right)^{0.5}, \tag{22}$$

where x is quality, μ_{L} and μ_{G} represent liquid and gas viscosities, respectively. Liquid and gas densities are denoted by ρ_{L} and ρ_{G}, respectively. In Eq. (21), the subscript LO corresponds to the value with the total flow in the liquid phase and the subscript c and s correspond to contraction and the smaller channel, respectively.

2.2. Non-circular micro-channels

Triplett et al. [6,7] also conducted the same systematic experiments as discussed in the previous section to study gas–liquid two-phase flow characteristics in semi-triangular micro-channels. The results obtained were similar to those obtained from circular channels.

Xu et al. [17] investigated an adiabatic co-current vertical two-phase flow of air and water in rectangular channels (12 mm × 260 mm) with mini-/micro-gaps of 0.3, 0.6 and 1.0 mm. For channel gaps of 1.0 and 0.6 mm, the flow patterns observed were similar to those found in ordinarily sized channels but peculiar flow structures which were different from typical two-phase flow patterns were observed in the channel having a micro-gap of 0.3 mm. In the 0.3 mm gap, they found that bubbly flow was never observed and new flow regimes including slug-droplet flow and annular-droplet flow were addressed. For the new flow regimes, it was observed that liquid droplets were always adhered to the wall surface and such droplets were blown by the moving gas phase. They also presented the models to predict the flow regime transitions in vertical rectangular channels. The models for bubbly flow to slug flow transition and slug flow to churn flow transition were developed based on Mishima and Ishii [18].

The transition from bubbly flow to slug flow is described by

$$j_{\mathrm{L}} = \left(\frac{1}{0.3C_{\mathrm{o}}} - 1\right)j_{\mathrm{G}} - \frac{0.35\sqrt{gD_{\mathrm{e}}}}{C_{\mathrm{o}}}, \tag{23}$$

where C_{o} is the distribution parameter and D_{e} represents the equi-periphery diameter and is given by

$$D_{\mathrm{e}} = \frac{2(s+w)}{\pi}, \tag{24}$$

where s and w are the channel gap and width, respectively. In Eq. (23), the distribution parameter, C_{o}, for rectangular channels is given by

$$C_{\mathrm{o}} = 1.35 - 0.35\sqrt{\frac{\rho_{\mathrm{G}}}{\rho_{\mathrm{L}}}}. \tag{25}$$

The slug-churn flow transition took place when

$$\alpha > \alpha_{\mathrm{m}}. \tag{26}$$

The void fraction, α, is given by

$$\alpha = \frac{j_G}{C_o(j_G + j_L) + V}, \tag{27}$$

where V is the rising bubble velocity relative to the liquid phase and is expressed by

$$V = 0.35\sqrt{gD_e}. \tag{28}$$

The slug bubble mean void fraction α_m, shown in Eq. (26), is defined as

$$\alpha_m = 1 - 0.813X^{0.75}, \tag{29}$$

where

$$X = \sqrt{\frac{\rho_L}{2g\,\Delta\rho L_B}}\left[(C_o - 1)(j_G + j_L) + 0.35\sqrt{gD_e}\right]. \tag{30}$$

L_B and $\Delta\rho$ are the slug bubble length and density difference between the two phases, respectively.

Based on a void fraction of 0.75, the transition of the annular flow took place when gas and liquid superficial velocities satisfied the following relationship:

$$1.33j_G - 4j_L = \sqrt{\frac{(\rho_L - \rho_G)gD_h + 128C_L\left(\frac{j_L D_h}{\nu_L}\right)^{-n_2}\rho_L j_L^2}{9.24C_G\left(\frac{D_h}{\nu_G}\right)^{-n_1}\rho_G\left[1 + 1.5\left(\frac{\rho_L}{\rho_G}\right)^{1/3}\right]}}\, j_G^{n_1/2}, \tag{31}$$

where C_L and C_G are dependent on the Reynolds number.

In Eq. (31), ν_L and ν_G, are kinematic liquid and gas viscosities, respectively. n_1 or n_2 is equal to unity for a laminar flow and n_1 or n_2 is equal to 0.25 for a turbulent flow. However, the models developed were found to be predictable for gaps larger than 0.6 mm. For the 0.3 mm micro-gap, they suggested that an appropriate theory consistent with peculiar flow regimes observed was needed to develop the flow regime transition models.

Zhao and Bi [19,20] performed experiments to study two-phase flow patterns in vertical upward air–water flow in equilateral triangular channels having hydraulic diameters of 2.886, 1.443 and 0.866 mm. The images of the flow patterns were taken by a high-speed motion analyzer along with the transient pressure-drop measurements. The flow patterns, including dispersed bubbly flow, slug flow, churn flow and annular flow, were observed in the two larger triangular channels. These observations were similar to those generally encountered in the ordinarily sized tubes placed in vertical direction. However, it was interesting to note that a new flow pattern, namely capillary bubbly flow, was identified in the smallest channel in addition to the typical flow patterns, excluding the dispersed bubbly flow. Another interesting point to note was that the slug–churn flow and churn–annular flow transition lines shifted to the right as the hydraulic diameter decreased. In addition, the previous flow regime transition models being available for upward gas–liquid two-phase flow in the ordinarily sized tubes could not be used to predict the flow transitions.

According to their second paper, the experimental investigation for analyzing gas velocity, void fraction, and pressure drop was carried out in the same experimental setup. They reported that, based on the distribution of the parameter suggested by Ishii [21] and based on negligible drift velocity, the drift-flux model was in reasonable agreement with the

experimental data for gas velocity obtained from all three test sections. In addition, they obtained a correlation for predicting the void fraction and single-phase pressure drop. The void fraction correlation developed was similar to that suggested by Armand and Treschev [11]. It was found that the Lockhart–Martinelli correlation was in good agreement with the two-phase pressure drop data when the proposed new single-phase friction factor correlation was employed.

Chung et al. [22] explored nitrogen gas–water two-phase flow characteristics in a square channel having a hydraulic diameter of 96 μm and compared the results with those for a 100 μm circular channel employed by Kawahara et al. [8]. Similar results including pressure drop and void fraction data were obtained, regardless of the channel geometry. In both channels, the Lockhart–Martinelli correlation appeared to do rather well when compared with the pressure drop data while the void fraction data were found to be in poor agreement with the homogeneous flow model as well as the Armand-type correlation. They also discussed the effect of channel shape on the transition boundaries for flow patterns observed.

A flow visualization study to clarify the flow patterns of vertical upward gas–liquid two-phase flow in rectangular mini-channels with hydraulic diameter ranging from 1.95 to 5.58 mm was carried out by Satitchaicharoen and Wongwises [23]. Air–water, air–20 wt% glycerol solution, and air–40 wt% glycerol solution were used as working fluids. In the experiments, they employed various rectangular test sections: 20 mm × 2 mm, 40 mm × 1 mm, 40 mm × 2 mm, 40 mm × 3 mm and 60 mm × 2 mm at an equal length of 1 m. The flow phenomena, which were bubbly flow, cap-bubbly flow, slug flow, churn flow and annular flow, were observed and recorded by a high-speed camera. The effects of gap size, channel width and liquid viscosity on the flow pattern transitions were discussed.

English and Kandlikar [24] carried out experiments to explore the effect of surfactants on two-phase pressure drop of air–water adiabatic flow in a 1 mm square channel. The conditions they tested were based on the operating control in a proton exchange membrane (PEM) fuel cell. The surfactant Triton™ DF-12 was employed to reduce the surface tension to 0.034 N/m. The application of the surfactant solutions appeared to have no effect on the pressure drop due to many possible reasons, such as characteristics of the flow pattern affecting interaction between the two phases, insufficient surface tension for an observable change, and temperature variation. The accuracy of existing models for two-phase pressure drop prediction was evaluated. Based on the Mishima and Hibiki model [25], English and Kandlikar [24] also developed a new model applicable to low mass fluxes, high mass qualities and annular flow by applying the Chisholm value for laminar–laminar flow of 5 instead of the original constant of 21.

Two-phase flow characteristics including flow pattern and pressure drop of ethanol–CO_2 flowing through a converging or diverging rectangular micro-channel were explored by Hwang et al. [26]. Different from previous works associated with the flow in micro-channels, they observed stratified wavy flows at the entrance of the converging micro-channel. Peculiar flow patterns and bubble interactions, which were due to the presence of pressure and acceleration effects in the variable cross-section channels, were also discussed. For the pressure drop, they found that the channel pressure drop in the diverging micro-channel was substantially small in comparison to that in the converging micro-channel. However, the two-phase frictional multiplier plotted against the Lockhart–Martinelli parameter for both channels was independent of the liquid flow rate. This result was in agreement with that observed in nitrogen–water two-phase flow in circular micro-channels investigated by Chung and Kawaji [12].

Due to different flow regimes raised in the same micro-channel under a given flow condition, Jassim and Newell [27] proposed void fraction and pressure drop models based on the probabilistic flow regime map. This modeling technique was developed in such a way that flow visualization data were incorporated into the models developed for predicting pressure drop as well as the void fraction for air–water at 20 °C and refrigerants including R410A and R134a at 10 °C with mass flux values ranging between 50 and 300 kg/m^2 s. A test section with 6-port micro-channels of 1.54 mm in hydraulic diameter was used to obtain time fraction data for different flow regimes including liquid, intermittent, annular, and vapor flows. The proposed probabilistic model for predicting total pressure drop in micro-channels can be expressed with many flow regime time fraction functions and is given by

$$\left(\frac{\mathrm{d}P}{\mathrm{d}z}\right)_{\mathrm{total}} = F_{\mathrm{liq}}\left(\frac{\mathrm{d}P}{\mathrm{d}z}\right)_{\mathrm{liq}} + F_{\mathrm{int}}\left(\frac{\mathrm{d}P}{\mathrm{d}z}\right)_{\mathrm{int}} + F_{\mathrm{vap}}\left(\frac{\mathrm{d}P}{\mathrm{d}z}\right)_{\mathrm{vap}} + F_{\mathrm{ann}}\left(\frac{\mathrm{d}P}{\mathrm{d}z}\right)_{\mathrm{ann}}, \tag{32}$$

where F_{liq}, F_{int}, F_{vap} and F_{ann} represent time fraction curve fits in liquid, intermittent, vapor and annular flow regimes, respectively. The pressure drop for single-phase flow, including that for liquid flow $(\mathrm{d}P/\mathrm{d}z)_{\mathrm{liq}}$ and that for vapor flow $(\mathrm{d}P/\mathrm{d}z)_{\mathrm{vap}}$, is determined from the conventional relation:

$$\left(\frac{\mathrm{d}P}{\mathrm{d}z}\right)_{\mathrm{liq\ or\ vap}} = f\frac{G^2}{2\rho}\left(\frac{1}{D_{\mathrm{h}}}\right), \tag{33}$$

where G is mass flux. The pressure drop model for intermittent flow assuming a homogeneous density, ρ_{T}, and employing the average kinetic energy, $\mathrm{KE}_{\mathrm{avg}}$, is given by

$$\left(\frac{\mathrm{d}P}{\mathrm{d}z}\right)_{\mathrm{int}} = 0.045\frac{1}{D_{\mathrm{h}}}\mathrm{KE}_{\mathrm{avg}},$$

where

$$\mathrm{KE}_{\mathrm{avg}} = \frac{G^2}{2\rho_{\mathrm{T}}}$$

and

$$\rho_{\mathrm{T}} = \left[\frac{x}{\rho_{\mathrm{G}}} + \frac{(1-x)}{\rho_{\mathrm{L}}}\right]^{-1}. \tag{34}$$

The annular flow pressure drop model is evaluated as follows:

$$\left(\frac{\mathrm{d}P}{\mathrm{d}z}\right)_{\mathrm{ann}} = \phi_{\mathrm{vo}}^2\left(\frac{\mathrm{d}P}{\mathrm{d}z}\right)_{\mathrm{VO}}, \tag{35}$$

where ϕ_{VO}^2 is two-phase multiplier and is expressed by

$$\phi_{\mathrm{VO}}^2 = \exp(-0.046X_{\mathrm{ann}}) + 0.22[\exp(-0.002X_{\mathrm{ann}}) - \exp(-7X_{\mathrm{ann}})], \tag{36}$$

$$X_{\mathrm{ann}} = \left[\left(\chi + \frac{1}{We_{\mathrm{v}}^{1.3}}\right)\left(\frac{\rho_{\mathrm{L}}}{\rho_{\mathrm{G}}}\right)^{0.9}\right], \tag{37}$$

where We_{v} in Eq. (37) represents the Weber number for vapor and is defined as

$$We_{\mathrm{v}} = \frac{\left[(xG)^2/\rho_{\mathrm{G}}\right]}{\sigma/D_{\mathrm{h}}}. \tag{38}$$

In Eq. (35), the vapor only pressure drop is given by

$$\left(\frac{\mathrm{d}P}{\mathrm{d}z}\right)_{\mathrm{VO}} = 2f_{\mathrm{VO}}\frac{1}{D_{\mathrm{h}}}\frac{G^2}{\rho_{\mathrm{G}}}. \tag{39}$$

The probabilistic void fraction model proposed is also expressed with many flow regime time fraction functions as shown by

$$\alpha_{\mathrm{total}} = F_{\mathrm{liq}}\alpha_{\mathrm{liq}} + F_{\mathrm{int}}\alpha_{\mathrm{int}} + F_{\mathrm{vap}}\alpha_{\mathrm{vap}} + F_{\mathrm{ann}}\alpha_{\mathrm{ann}}, \tag{40}$$

where α_{liq} represents the void fraction for liquid only flow and is equal to 0, while α_{vap} represents the vapor only flow void fraction which is equal to 1. The intermittent flow void fraction, α_{int}, and annular flow void fraction, α_{ann}, are defined as follows:

$$\alpha_{\mathrm{int}} = \frac{(0.833 + 0.167x)x\left(1/\rho_{\mathrm{G}}\right)}{(1-x)\left(1/\rho_{\mathrm{L}}\right) + x\left(1/\rho_{\mathrm{G}}\right)}, \tag{41}$$

$$\alpha_{\mathrm{ann}} = \left[1 + \left(\chi + \frac{1}{We_{\mathrm{v}}^{1.3}}\right)\left(\frac{\rho_{\mathrm{L}}}{\rho_{\mathrm{G}}}\right)^{0.9}\right]^{-0.06}. \tag{42}$$

Pressure drop and void fraction predictions based on the probabilistic flow regime map were found to be in accordance with the measured data obtained in micro-channels. However, care should be taken when the models are needed to be applied under conditions and geometries other than those in which the probabilistic flow regime maps were established.

3. Conclusions

As discussed above, this review reveals that there is only a small amount of publications available for the two-phase gas–liquid adiabatic flow in micro-channels. The existing literature is still lacking in various aspects, including geometry of mixing chamber configuration, fluid properties, channel orientation and relevant flow models.

It is obvious that the status of current researches on phase-change heat transfer and two-phase flow phenomena in micro-channels is still in infant stage and a great deal of systematic investigations will become substantially more necessary to meet general conclusions needed for the appropriate design and process control of several engineering applications.

Acknowledgements

The authors would like to express their appreciation to the Thailand Research Fund (TRF) and the Joint Graduate School of Energy and Environment (JGSEE) for providing financial support for this study.

References

[1] Serizawa A, Feng Z, Kawara Z. Two-phase flow in micro-channels. Exp Therm Fluid Sci 2002;26:703–14.
[2] Suo M, Griffith P. Two-phase flow in capillary tubes. J Basic Eng 1964;86:576–82.
[3] Brauner N, Moalem-Maron D. Identification of the range of small diameter conduits regarding two-phase flow pattern transitions. Int Commun Heat Mass Transfer 1992;19:29–39.
[4] Mehendale SS, Jacobi AM, Ahah RK. Fluid flow and heat transfer at micro- and meso-scales with application to heat exchanger design. Appl Mech Rev 2000;53:175–93.
[5] Kandlikar SG. Fundamental issues related to flow boiling in mini-channels and micro-channels. Exp Therm Fluid Sci 2002;26:389–407.
[6] Triplett KA, Ghiaasiaan SM, Abdel-Khalik SI, Sadowski DL. Gas–liquid two-phase flow in microchannels Part I: two-phase flow patterns. Int J Multiphase Flow 1999;25:377–94.
[7] Triplett KA, Ghiaasiaan SM, Abdel-Khalik SI, LeMouel A, McCord BN. Gas–liquid two-phase flow in microchannels Part II: void fraction and pressure drop. Int J Multiphase Flow 1999;25:395–410.
[8] Kawahara A, Chung PM-Y, Kawaji M. Investigation of two-phase flow pattern, void fraction and pressure drop in a microchannel. Int J Multiphase Flow 2002;28:1411–35.
[9] Chen WL, Twu MC, Pan C. Gas–liquid two-phase flow in micro-channels. Int J Multiphase Flow 2002;28:1235–47.
[10] Zhao L, Rezkallah KS. Gas–liquid flow patterns at micro-gravity conditions. Int J Multiphase Flow 1993;19:751–63.
[11] Armand AA, Treschev GG. Izv Vses Teplotek Inst 1946;1:16–23.
[12] Chung PM-Y, Kawaji M. The effect of channel diameter on adiabatic two-phase flow characteristics in microchannels. Int J Multiphase Flow 2004;30:735–61.
[13] Garimella S, Killion JD, Coleman JW. An experimentally validated model for two-phase pressure drop in the intermittent flow regime for circular microchannels. J Fluids Eng-Trans ASME 2002;124:205–14.
[14] Coleman JW, Krause PE. Two phase pressure losses of R134a in microchannel tube headers with large free flow area ratios. Exp Therm Fluid Sci 2004;28:123–30.
[15] Schmidt J, Friedel L. Two-phase pressure drop across sudden contractions in duct areas. Int J Multiphase Flow 1997;23:283–99.
[16] Abdelall FF, Hahn G, Ghiaasiaan SM, Abdel-Khalik SI, Jeter SS, Yoda M, et al. Pressure drop caused by abrupt flow area changes in small channels. Exp Therm Fluid Sci 2005;29:425–34.
[17] Xu JL, Cheng P, Zhao TS. Gas–liquid two-phase flow regimes in rectangular channels with mini/micro gaps. Int J Multiphase Flow 1999;25:411–32.
[18] Mishima K, Ishii M. Flow regime transition criteria for upward two-phase flow in vertical tubes. Int J Heat Mass Transfer 1984;27:723–37.
[19] Zhao TS, Bi QC. Co-current air–water two-phase flow patterns in vertical triangular micro-channels. Int J Multiphase Flow 2001;27:765–82.
[20] Zhao TS, Bi QC. Pressure drop characteristics of gas–liquid two-phase flow in vertical miniature triangular channels. Int J Heat Mass Transfer 2001;44:2523–34.
[21] Ishii M. One-dimensional drift-flux model and constitutive equations for relative motion between phases in various two-phase flow regimes. ANL Report ANL-77-47, 1977.
[22] Chung PM-Y, Kawaji M, Kawahara A, Shibata Y. Two-phase flow through square and circular microchannels—effects of channel geometry. J Fluids Eng-Trans ASME 2004;126:546–52.
[23] Satitchaicharoen P, Wongwises S. Two-phase flow pattern maps for vertical upward gas–liquid flow in mini-gap channels. Int J Multiphase Flow 2004;30:225–36.
[24] English NJ, Kandlikar SG. An experimental investigation into the effect of surfactants on air–water two-phase flow in minichannels. In: Proceedings of the ICMM2005 third international conference on microchannels and minichannels, Toronto, Ont., Canada, June 13–15, 2005. p. 1–10.
[25] Mishima K, Hibiki T. Some characteristics of air–water two-phase flow in small diameter vertical tubes. Int J Multiphase Flow 1996;22:703–12.
[26] Hwang JJ, Tseng FG, Pan C. Ethanol–CO_2 two-phase flow in diverging and converging microchannels. Int J Multiphase Flow 2005;31:548–70.
[27] Jassim EW, Newell TA. Prediction of two-phase pressure drop and void fraction in microchannels using probabilistic flow regime mapping. Int J Heat Mass Transfer 2006;49:2446–57.